Health Impacts of PM Emissions from Passenger Cars in Europe and Reduction Potentials due to Electric Vehicles

Thomas Heck

Laboratory of Energy Systems Analysis, Paul Scherrer Institut, 5232 Villigen, Switzerland, thomas.heck@psi.ch

Abstract

The present paper investigates the potential influence of electric vehicles on PM (particulate matter) emissions in Europe with a special focus on the potential reduction of non-exhaust emissions due to electric braking. The associated health impacts are estimated. In order to improve the impact assessment, two new methods are proposed: a) an analytical approximation of the spatial distribution of cars in Europe which is in particular useful to set up future scenarios with few parameters, and b) an analytical approximation for space-dependent impact assessment that is adjusted to available statistical data and simple enough for practical applications (e.g. for space-dependent life cycle impact assessment).

Introduction

In the past, particulate emissions from cars have been dominated by exhaust emissions. Due to consecutive emission regulations, PM (particulate matter) exhaust emissions of passenger cars in Europe have been reduced. During the same time, the non-exhaust emissions due to brakes, tires and road abrasion have increased because of the increasing number of passenger cars and vehicle-kilometres driven. Today, non-exhaust PM_{10} (i.e. PM size≤10µm) emissions are approximately on the same level as primary PM_{10} exhaust emissions of passenger cars in Europe. The introduction of the new Euro-6 emission norm is intended to reduce exhaust PM emissions further in future. Studies commonly assume a further increase of car traffic in Europe. Thus it can be expected that direct primary PM_{10} emission will be dominated in future by non-exhaust emissions.

The introduction of a high share of electric cars in the fleet would have two effects on the direct PM emissions: On the one hand, pure electric vehicles (or hybrids in the phase of electric driving) have no combustion-related exhaust emissions. On the other hand, electric and hybrid-electric vehicles can also lead to a reduction of non-exhaust emissions because a part of the friction braking is replaced by electric braking without abrasion.

Figure 1 shows projections of direct primary PM_{10} emissions from passenger cars in Europe (EU-27) until 2050 (details are explained below). A medium demand scenario is assumed i.e. a moderate increase of passenger cars and vehicle-kilometres driven during the projection period. In the BAU (business-as-usual, red curves) projection, it is assumed that the fleet will remain almost exclusively based on fossil fuel together with the spreading of strict emission limits and the step-by-step removal of old cars. The exhaust emissions (dashed) will be reduced due to new emission regulations but the non-exhaust emissions (dotted) will significantly increase. The solid curve on top shows the sum of exhaust and non-exhaust emissions.

A strong penetration of electric vehicles (EV) into the European market (green curves) leads to a further decrease of exhaust emissions but also to a reduced increase of non-exhaust emissions compared to BAU. Both contributions of electric vehicles to the PM_{10} reduction are in the same order of magnitude.

The environmental overall balance depends also on the life cycle contributions i.e. on the indirect emissions due to the fuel cycle and the life cycle of the vehicles. For electric mobility, the total PM emissions depend also significantly on the electricity generation technologies chosen for the future electricity supply.

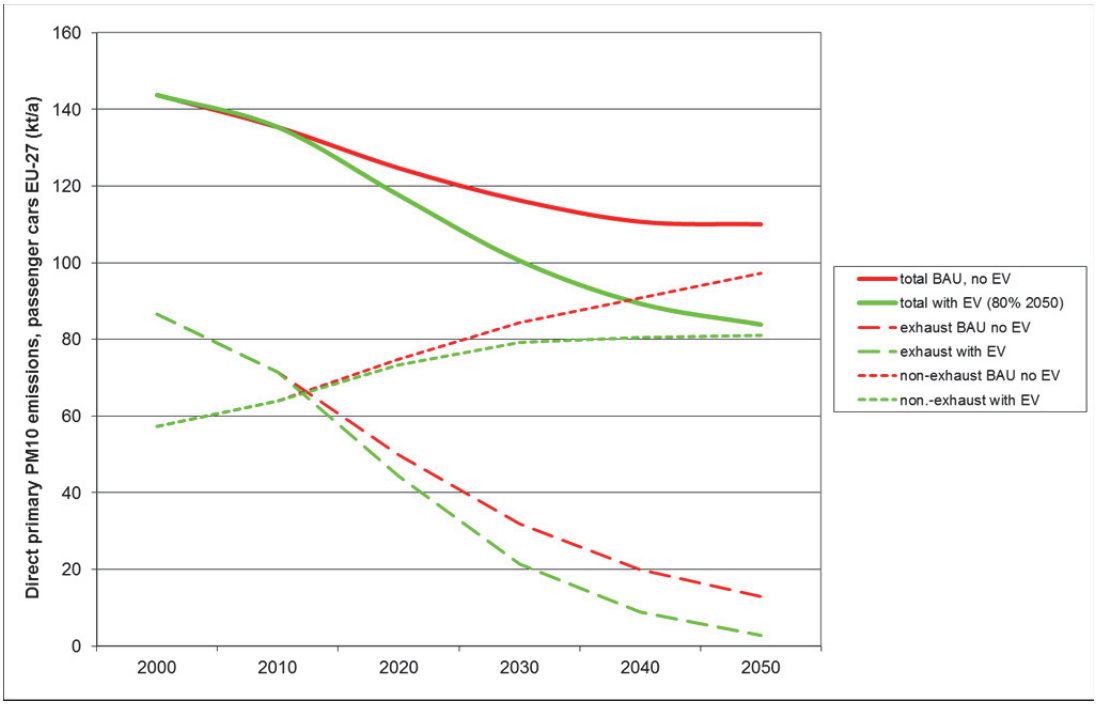

Figure 1: Projections of direct primary particulate matter (PM10) emissions from passenger cars in EU-27 (kt/a) until year 2050.

Based on the emission scenarios, the health impacts are estimated using environmental impact assessment methods.

Methods

The methods are based on the impact pathway approach developed within the European projects ExternE (Holland et al. 1999; Friedrich and Bickel 2001; Bickel et al. 2005) and NEEDS (NEEDS 2009), and the ongoing Swiss THELMA project (www.thelma-emobility.net). For life cycle contributions, the ecoinvent life cycle database (Ecoinvent 2010) is used.

Figure 2 shows the principle of the impact pathway model, coupled to the life cycle database, including a valuation step.

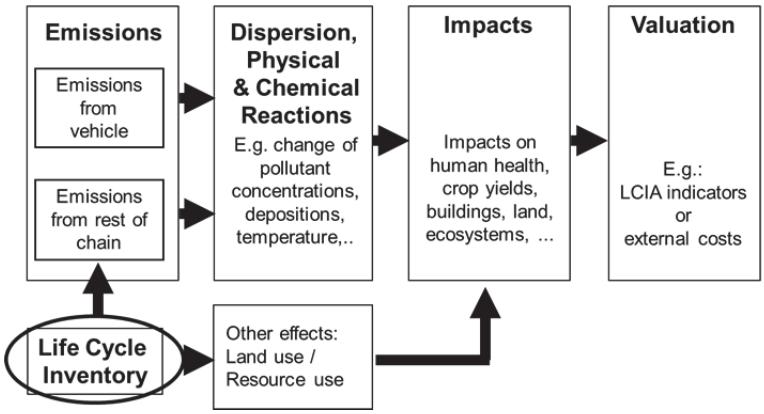

Figure 2: Principle of the impact pathway approach.

The basic approach is the bottom-up environmental impact and external costs assessment in combination with life cycle inventory (LCI) data. Conventional life cycle impact assessment (LCIA) does not consider the locations of emissions. However, environmental impacts like PM health damages depend significantly on the emission location (Krewitt et al. 2001; Heck and Hirschberg 2011). In the “semi-regionalized approach” (Heck and Meyer 2010) the contributions to environmental burdens are split into two parts: Most important emission sources with known locations are modeled with site-specific impact assessment methods. Less important emissions sources or sources where locations are unknown are treated with constant impact factors (like in traditional life cycle impact assessment). The semi-regionalized approach is a compromise between detailed modeling and simplification due to limited data availability.

The focus of the present paper is on the health impacts of particulate matter (PM) emissions from passenger cars. Several epidemiological studies show a connection between particulate matter in the air and impacts on human health e.g. (Ostro 1987; Dockery et al. 1993; Abbey et al. 1995; Xu 1998; Laden et al. 2000; Brunekreef and Holgate 2002; Pope III and Dockery 2006; Götschi et al. 2008; Pope III et al. 2009; Schindler et al. 2009). The impacts include a couple of diseases like chronic bronchitis or asthma but also the increase of mortality i.e. the reduction of life expectancy. Fine particulate matter in the air increases for example the risk of lung cancer (Raaschou-Nielsen et al. 2013). The major health indicator used here is "Years of Life Lost" (abbreviated in literature as YOLL or YLL) i.e. the reduction of life expectancy summed over the affected population. A recent European study (Beelen et al. 2014) showed an increase of mortality risk due to long-term PM2.5 exposure not only for high but also for low annual mean concentrations below 20 µg/m3 and thus well below the European legal limit of 25 µg/m3.

The modelling is based on the ExternE EcoSense model which combines environmental impact and external cost assessment (Heck et al. 1999; Droste-Franke et al. 2004; Bickel et al. 2005). The major air quality modeling grid is based on the EMEP 50 km x 50 km grid covering the whole of Europe (EMEP 1996). The EcoSense model employs the Windrose Trajectory Model (Trukenmüller and Friedrich 1995), which is based on the Harwell Trajectory model (Derwent and Nodop 1986). WTM is a Lagrangian trajectory model calculating changes of concentrations and depositions. Besides the dispersion of primary particulates, it includes the formation of secondary particulates from sulfur dioxide, nitrogen oxides and ammonia emissions. The impacts of regional air pollution are summed up over all grid cells of the impact assessment area.

Passenger transport is correlated to the spatial population distribution. Thus, the use of a 50 km x 50 km grid alone is not satisfactory in particular for primary particulate emissions because the correlations inside a grid cell are lost. Detailed impact models for transport have been developed to improve the estimates (e.g. (Friedrich and Bickel 2001; Schmid 2005; Jensen et al. 2008)), in particular for urban areas (Moussiopoulos et al. 2012; Torras Ortiz 2012; Torras Ortiz and Friedrich 2013). The disadvantage of detailed models is that they usually need a lot of local data and thus in practice only few specific locations have been investigated in detail. For simplification, the linearity of health-impact functions was already used in the uniform world model (Curtiss and Rabl 1996) and variants (Spadaro 1999). Another simplifying approach for road transport is the use of few classes like only two emission location types ("built-up areas" and "non-built-up areas") used in (VSS 2009). The large difference for PM implies a big discontinuity depending on whether a location is classified as "built-up" or "non-built-up".

The intention of the present study is to improve the modeling for averages over larger areas by considering the correlations between traffic and population distribution. The proposed model interpolates between local analytical models and numeric calculations covering local and regional scales. Analytical approximations for exposure integrals are discussed. The model refers mainly to PM emissions near ground, but more general cases are discussed briefly.

Emission scenario modelling

The total annual kilometers traveled in a country or in the whole of Europe can be estimated from the total annual consumption of fuel (e.g. petrol) based on sales volumes, the total number of cars, the average mileage per car and the average consumption per vehicle-km (e.g. (DIW 2012)). Data on the performance in terms of passenger-kilometers (pkm) per country are available from Eurostat (Eurostat 2012). Emission factors are usually given per vehicle-km (vkm). The demand of passenger car transport is expected to grow significantly in Europe, in particular in those countries which currently still have less cars per person than the average EU. For the calculation in this paper, medium demand estimates of total pkm until 2050 in (Skinner et al. 2010) have been used. For the conversion, 1.6 pkm/vkm was assumed (Spielmann et al. 2007). Assumptions here: ca. 2.7E+12 vkm/a in 2000, ca. 4.6E+12 vkm/a in 2050.

Emission factors for vehicles have been collected from different sources (EMEP/CORINAIR 2007; BAFU 2010; Ecoinvent 2010; Simons 2013). Assumptions for non-exhaust emissions of conventional cars in mg/vkm PM_{10} ($PM_{2.5}$) are: tires 6.4 (4.5), brakes 7.3 (2.9), road 7.5 (4.1), based on (EMEP/CORINAIR 2007).

Other estimates of brake wear emissions showing the ranges are e.g.: PM_{10} ~5 mg/vkm, 75% $PM_{2.5}$ (Boulter 2005); PM 5.1-14.1 mg/mile (86% PM_{10}, 63% $PM_{2.5}$) median value 6.2 mg/mi $PM_{2.5}$ (Garg et al. 2000); brake wear from small vehicles 5 mg/mi PM_{10} (Cadle 2004). Measurements in Zürich together with Positive Matrix Factorization yielded 8+-4 mg/vkm PM_{10} for brake wear from light vehicles, including delivery vans (Bukowiecki et al. 2009). For heavy vehicles, the emission factors for brake abrasion were about a factor 10 higher than for light vehicles.

The spatial distribution of the emissions from traffic is a separate issue and will be discussed in an own section (see below).

Figure 3 shows the results of a BAU future transport scenario for primary particulate emissions up to the year 2050, assuming no EV market penetration.

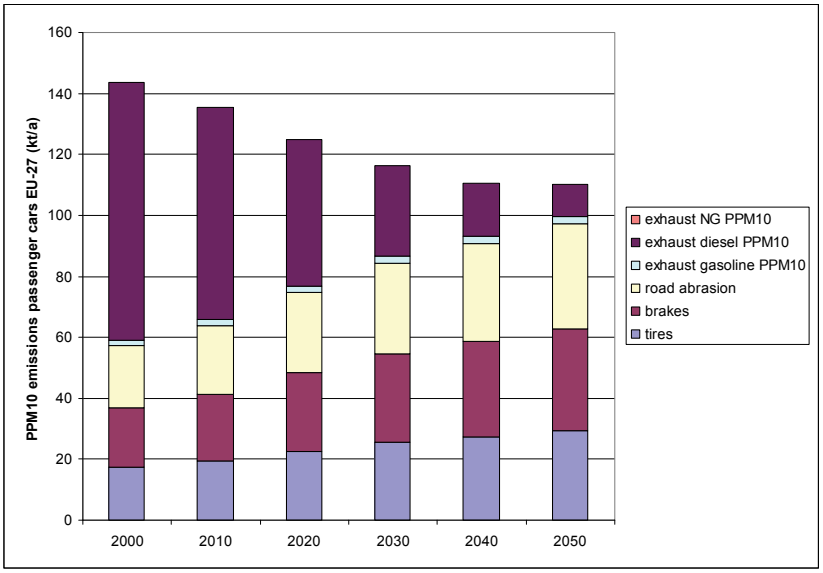

Figure 3: Reference scenario for primary PM10 emissions of passenger cars in Europe EU-27, 2000 – 2050 (no electric vehicles, direct emissions only).

Potential emission reduction due to electric braking

Figure 4 shows an example for the speed, power and energy during the braking phase of a vehicle from 120 km/h to full stop with a strong deceleration during the initial phase and, after about 10s, a soft end-phase during about 5s. (Assumed mass 1600kg, drag coefficient c_w=0.28, cross-sectional area 1.9m^2, rolling resistance ca. 0.01 speed-dependent (Gollnick 2004)). At the beginning, a braking power of about 160 kW is needed. The power of the electric brakes is assumed to be limited to 40 kW acting at all four wheels together, so that 75% of braking power must be taken by the friction brakes at the beginning. The use of the friction brakes implies emissions of non-exhaust PM. When the speed decreases, the braking power decreases and more and more can be taken over by the electric brakes. In the last phase, the friction brakes have to be activated until full stop but this slow phase is associated with only low power. The red curve shows the cumulative friction braking energy of a conventional car without electric brakes, the green curve shows the corresponding remaining friction energy of a car with 4-wheels electric braking. The PM emissions are assumed to be proportional to the energy absorbed by the friction brakes. In the example, the electric brake can take about 45% of the braking energy. Thus the potential reduction of PM brake emissions is about 45% in this example (which will be called “120stop10s+5s”).

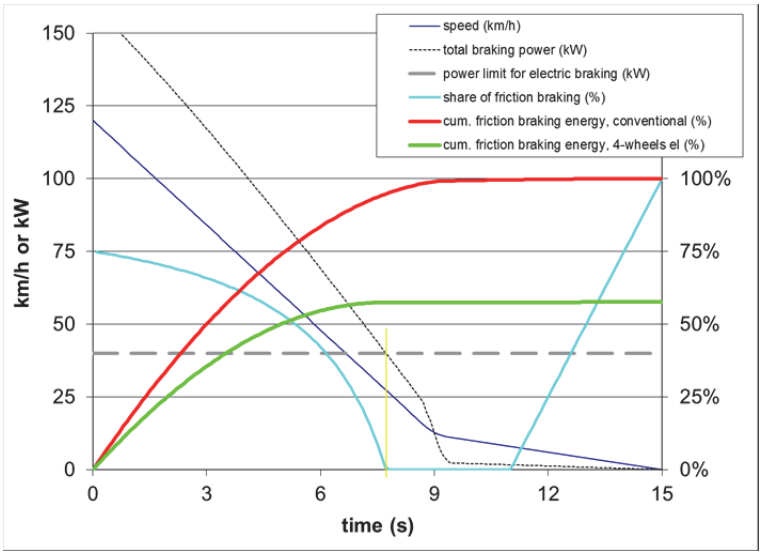

Figure 4: Braking phase of a car (parameters in text) beginning at a speed of 120 km/h.

The same calculation was applied to several driving cycles (New European Driving Cycle NEDC, US-EPA FTP, World Light Test Procedure WLTP, Artemis (Andre 2004)) for a medium size car. **Figure 5** shows the results depending on the power of the electric brake.

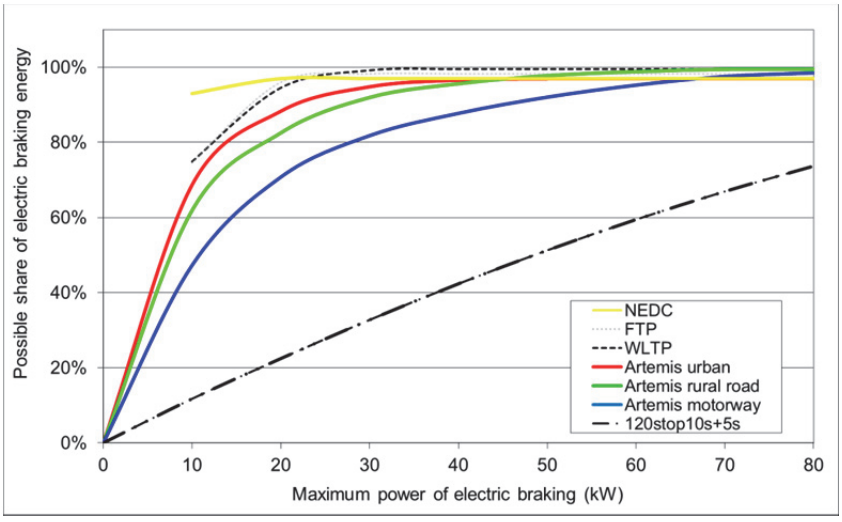

Figure 5: Possible share of electric braking energy for different driving cycles depending on the maximum braking power a 4-wheels electric braking system can provide.

The potential reduction is >80% for the full cycles above an electric power of 30 kW. Nevertheless, note that this refers to idealized conditions and electric brakes at all 4 wheels. Usually, the front wheels take about 2/3, the rear wheels about 1/3 of braking power. Thus if, for safety reasons, braking must apply to all 4 wheels, electric or hybrid cars with electric brakes at 2 wheels only have lower reduction potentials depending on the positioning. Thus the medium reduction potential of brake wear emissions per car is assumed at 60% (high 90%, low 30%). The resulting scenario for a strong market penetration of 80% electric vehicles until year 2050 with medium assumptions is shown in **Figure 1**.

Approximate spatial distribution of cars in Europe - a new analytical approach

Figure 6 shows the correlations between population density and stock of passenger cars for different European countries. Data are derived from the stock of cars on NUTS (Nomenclature of Units for Territorial Statistics) level 2 (Eurostat 2014) and from Swiss Federal Office of Statistics (canton level) (BfS 2012). Data refer to year 2010 (for some lacking data: 2008-2009). Only countries for which at least 8 or more data points for the stock of cars were available from the eurostat database were considered (with the exception of Switzerland for which detailed data from national statistics were available). The total number of cars per 1000 people in a country depends on the income level, therefore the trend lines are calculated separately for the different countries.

The car stock data as functions of population density show a "fan-shaped" structure (**Figure 6**): In countries with low income/capita and a low total number of cars per 1000 persons, the stock of cars tends to increase with population density of the area. By contrast, countries with high total number of cars and higher income/capita show a decrease of car stock per 1000 persons with increasing population density. Most of the trend lines intersect roughly in the region of 500 cars per 1000 persons and 500-1000 persons per km^2.

How can this "fan-shaped" pattern be explained? In countries with low average income/capita, people living in the relatively prosperous metropolitan areas are often the first who can afford a car. Consequently, the stock of cars tends to be concentrated in the highly populated areas. By contrast, the city areas in countries with high income/capita usually offer enough alternative transportation opportunities in terms of public transportation or vehicles for hire (taxis, car rental, car sharing etc.). Furthermore, congestion and shortage of parking space limit the benefit of car driving in big cities. In high-income countries, people living on the countryside tend to have most cars because the conditions for cars are attractive (enough parking space, good roads) whereas the connection to trains or other public transportation in the rural areas is worse than in the well-connected cities. Simply summarized, metropolitan areas in lower-income countries tend to "attract" car traffic, whereas metropolitan areas in higher-income countries tend to "repel" car traffic due to saturation and by providing attractive alternatives.

The "fan-shaped" pattern suggests the following approach for parameterization:

$$q(x) = \max(0, q_c - a \cdot (q_c - q_0) \cdot \ln\left(\frac{\min(p(x), p_l)}{p_0}\right) / (1 + \exp((q_{crit} - q_c) \cdot w)) \qquad (1)$$

Here, x denotes the location of the considered local area (e.g. NUTS2, NUTS3 or NUTS5/LAU2 area), p(x) is the population density in area x, q_c is the average number of cars per 1000 persons in country c, q(x) is an estimate of the number of cars per 1000 in area x. The parameters a, q_0, p_0, q_{crit}, and w are adjusted to the available data. The function is set constant above a certain population density p_l.

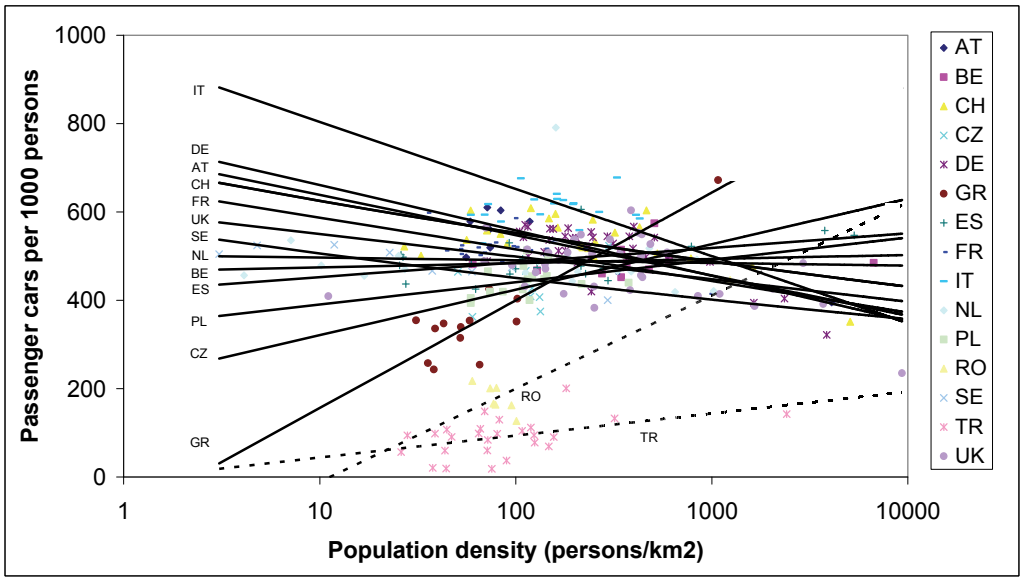

Figure 6: The "fan-shaped" set of trend lines for the relationship between population density and stock of passenger cars in different European countries (logarithmic fit).

Figure 7 shows the set of curves according to equation (1) for the parameters a=0.58, q_0=481, p_0=300, q_{crit}=240, w=0.02, p_l=p_0*exp(1/a), which approximate the set of curves in **Figure 6**.

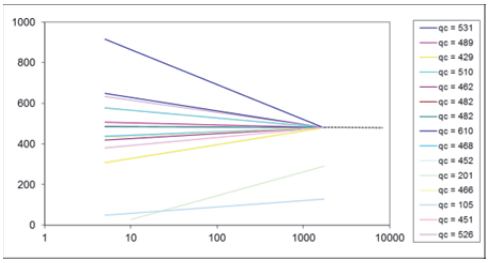

Figure 7: Parameterized set of functions

Finally, the q(x) are scaled so that the sum of q(x)*Population(x)/1000 matches the country total q_c*Population/1000, or, if available, the totals within a more detailed resolution for which averages are given (e.g. NUTS2 units).

The advantage of the parameterization (1) is that it can be used to generate easily an approximate spatial distribution for future scenarios. It can be expected that the distribution within countries which have currently only few cars per person will develop with increasing car stock in a similar way as in countries which have already today a high number of cars because the principle issues are the same (limited space in densely populated areas, less public transportation possibilities in sparsely populated country-side areas compared to metropolitan areas).

The average number of cars per 1000 persons q_c in a country is related to the income level of the country. A regression with data from (Eurostat 2014)(nama_r_e2gdp, tran_r_vehst) for the 30 countries available for 2010/2011 (AT, BE, BG, CH, CY, CZ, DE, DK, EE, EL, ES, FI, FR, HR, HU, IE, IT, LT, LU, LV, MT, NL, NO, PL, RO, SE, SI, SK, TR, UK) yields the approximation q_c=110*(ln(GDP_{Cap}/371Euro)) where GDP_{Cap} is the gross domestic product per capita in country c in current Euro (R^2=0.432). The GDP growth can be used to scale up approximately the car stocks and vkm for future scenarios. Political goals (e.g. for car traffic limitation) can be considered by adjusting the parameters.

For the present calculations, the sums of the relative distributions have been adjusted to the total km scenario values (see above).

A new approximation approach for spatially resolved impact assessment

When considering mobile emission sources, it should be kept in mind that in principle also the receptors are mobile. In an idealized model for mobile receptors, the expectation value of the impact on an individual k at time t would be written as

$$\left\langle I_k(t)\right\rangle = \int_{t_0}^{t} F_k(\tau, c(\vec{x}_k(\tau),\tau))d\tau \tag{2}$$

where $\vec{x}_k(\tau)$ describes where the individual k stayed at time τ, c is the pollutant concentration, F_k are health damage functions considering e.g. the age of the person. The time integration is taken over the whole lifetime until t. The total impacts are calculated by summing up over k. In a Lagrangian dispersion model, the mean concentration depending on mobile emission sources i.e. the fleet of vehicles v each of which is described by its time-dependent position $\vec{x}_v(t')$ and emission rate $e_v(t')$ would be (S_0 describes the other background emissions, δ is the Dirac delta function; insert the mobile sources into eq. (18.8) in (Seinfeld and Pandis 2006)):

$$\begin{aligned}\left\langle c(\vec{x},\tau)\right\rangle = &\int_{-\infty}^{\infty}\int_{-\infty}^{\infty}\int_{-\infty}^{\infty} Q(\vec{x},\tau|\vec{x}_0,t_0)\left\langle c(\vec{x}_0,t_0)\right\rangle d^3x_0 \\ &+\int_{-\infty}^{\infty}\int_{-\infty}^{\infty}\int_{-\infty}^{\infty}\int_{t_0}^{\tau} Q(\vec{x},\tau|\vec{x}',t')\left(S_0(\vec{x}',t')+\sum_v e_v(t')\delta(\vec{x}'-\vec{x}_v(t'))\right)dt'd^3x'\end{aligned} \tag{3}$$

In practice, simplifications have to be made.

For a non-threshold approach with linear exposure-response function, the concentration <c> is usually averaged over a long time unit (e.g. one year), and the damage functions are given in terms of impacts per time unit (e.g. cases per year) as (c.f. (Holland et al. 1999))

$$\frac{dI}{dt} = f_{er}\cdot\int_{-\infty}^{\infty}\int_{-\infty}^{\infty} p(x,y)\cdot\left\langle c(x,y,z=const)\right\rangle dxdy \tag{4}$$

This has been the basis for extensive numeric models. The exposure-response factors f_{er} are constants depending on the pollutant (e.g. the size of the particles), the impact and the risk group (Holland et al. 1999; Hurley et al. 2005; Torfs et al. 2007). The population density p(x,y) is commonly derived from statistics on the usual resident population. A split into a local and a regional area was made already in the EcoSense model (ISC and WTM, see e.g. Krewitt et al. 2001), and in improved uniform world models using areas of constant population density (Curtiss and Rabl 1996; Spadaro 1999) mainly for stack emissions. In both cases, the local area is relatively large (order of 50 km from source). The following approximation is derived more explicitly, covers a wider range of local area sizes, is applicable to low emission sources and adjusted to available statistical data (generalizations briefly discussed in the appendix).

Consider a partition of the total region (e.g. the whole of Europe) in smaller areas $\mathbf{A}_n$ (e.g. administrative units NUTS, or land use data) so that the time-averaged population density within each area $\mathbf{A}_n$ is approximately a constant $p(\mathbf{A}_n)$. $p(\mathbf{A}_{n,r})$ be the population density of the surrounding region $\mathbf{A}_{n,r}$ (e.g. the rest of the country to which the administrative unit $\mathbf{A}_n$ belongs).

The simplest approximation derived in the appendix yields for the impact I per emissions mass unit m emitted in area $\mathbf{A}_n$ (area size A_n) with parameters ϕ>0, κ>0, A_0>0:

$$\frac{I}{m} \approx \phi \cdot \left(p(\mathbf{A}_{n,r}) + (p(\mathbf{A}_n) - p(\mathbf{A}_{n,r})) \cdot \min\left(1, \left(\frac{A_n}{A_0}\right)^{\frac{\kappa}{2}}\right)\right) \tag{5}$$

The simplest choice for κ is κ=1/2 (see appendix). Generally, the parameters ϕ, κ and A_0 depend on the detailed model assumptions. The reference area A_0 depends on wind speed, deposition velocity and emission height. Actually, the parameters have to be adjusted to results of detailed simulations.

Figure 8 shows results from several detailed model runs ((Friedrich and Bickel 2001; Krewitt et al. 2001; Jensen et al. 2008); own calc.) adjusted to the recent exposure-response function for average $PM_{2.5}$. The approximate linearity holds from country areas (blue) down to relatively small administrative unit areas of 100-200km^2 for road transport emissions. The trend line yields a lower estimate for the parameter ϕ_{min}≈1.2YOLL/kt$PM_{2.5}$ per persons/km^2, because the numeric calculations include local and regional impacts.

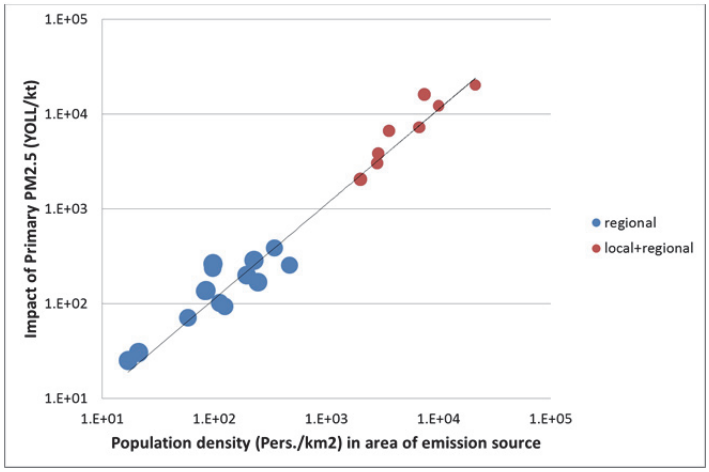

Figure 8: Health impacts in terms of Years of Life Lost per kilo-ton average PM2.5 emitted depending on population density based on different studies. The size of a bubble is proportional to the logarithm of the area of the administrative unit of emission.

The proposed approximation formula can be applied in principle to emission areas of arbitrary size as long as reasonable values for the exponent κ are used. If the size of the emission area exceeds the reference area parameter A_0, the damages are dominated by the local area i.e. the local population density. If the emissions area A_n is smaller than A_0, a substantial part of the pollutants leaves the area $\mathbf{A}_n$ and the total damage consists of contributions of $\mathbf{A}_n$ and the surrounding region $\mathbf{A}_{n,r}$. The contribution of the local area tends to zero if the size of the local area tends to zero. Thus the formula interpolates continuously between small and large areas.

If the impact factor $d_{n,\rho}$ for the greater region $\mathbf{A}_{n,\rho}$ containing $\mathbf{A}_n$ (e.g. the country of $\mathbf{A}_n$), is already given based on regional geographical information, the formula can be modified to provide a local correction as (note that $A_{n,\rho}$= A_n + $A_{n,r}$):

$$\frac{I}{m} \approx d_{n,\rho} \cdot \left(1 + \frac{(p(\mathbf{A}_n) - p(\mathbf{A}_{n,\rho}))}{p(\mathbf{A}_{n,\rho})} \cdot \min\left(1, \left(\frac{A_n}{A_0}\right)^{\frac{\kappa}{2}}\right)\right) \tag{6}$$

The proposed approximation method uses primarily local population densities and area sizes i.e. data that is generally available in statistical databases and thus can be used to cover a large impact assessment region. The possibility to use the same spatial resolution like for the emission sources compensates somewhat for the disadvantage of not following the detailed movements of sources and receptors: if a lot of cars move during the day from region A to B, also a substantial part of the population moves from A to B keeping the correlation at least partly.

Results for health impacts

Figure 9 shows the scenario results for health impacts of direct primary particulate emissions of passenger cars in Europe EU-27 in terms of Years of Life Lost per year. The corresponding emissions are shown in **Figure 1** above. In terms of PM10 emissions, non-exhaust emissions strongly dominate the totals in year 2050. By contrast, the relative contribution of non-exhaust emissions to health impacts is weaker because of the size distribution (PM2.5 has higher impacts than larger size fractions) and the assumed higher toxicity of exhaust emissions. For the same reason, the reduction of health impacts of direct primary PM emissions in the electric vehicle scenario compared to the BAU scenario in 2050 is expected to be slightly dominated by exhaust emissions (green curves versus red curves in **Figure 9**), whereas non-exhaust emissions contribute about half to the PM10 reductions of the electric car scenario compared to the BAU scenario (**Figure 1**). Nevertheless, non-exhaust emissions are expected to dominate also the health impacts of direct primary PM emissions in 2050. The current health impacts due to direct primary PM emissions are estimated at about 130'000 YOLL/a based on medium assumptions on NUTS3 level (absolute numbers have high uncertainties).

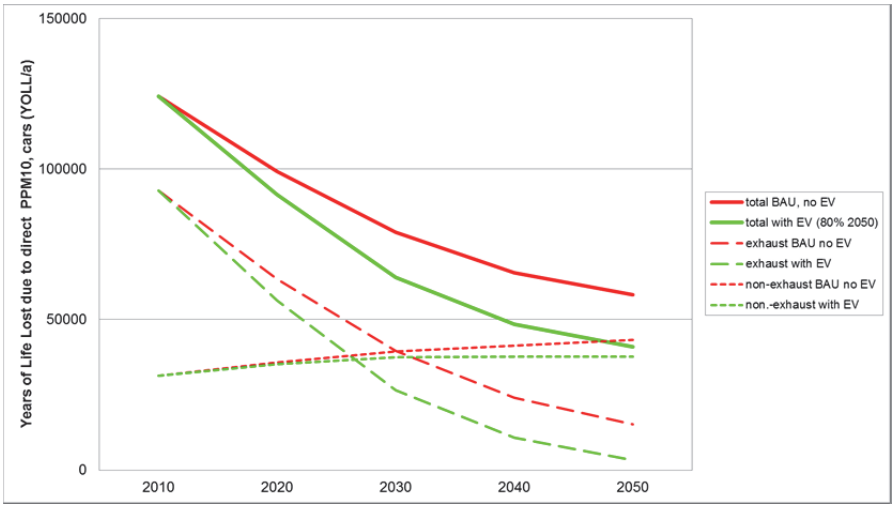

Figure 9: Estimated health impacts in terms of Years of Life Lost per year for EU-27 passenger car scenarios.

The focus of the present paper was on the primary PM emissions from the cars. **Figure 10** shows the contributions of direct primary and secondary PM from the vehicles together with indirect contributions from the rest of chain for different conventional cars (emission norms Euro-I for old cars to Euro-VI for advanced car technology) compared to electric cars (secondary organic aerosols are not included). The shown set refers to Swiss conditions. For comparison, also an electric car supplied by electricity from coal UCTE mix (Ecoinvent 2010) is included. The comparison shows the strong dependency of overall impacts of electric cars on the electricity supply.

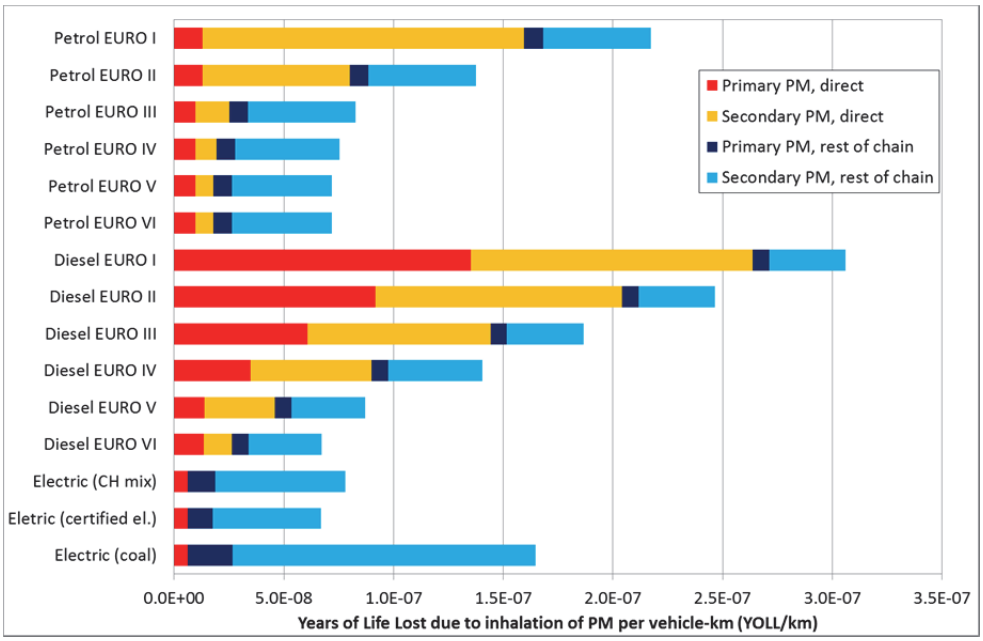

Figure 10: Estimated health impacts due to inhalation of PM in terms of YOLL per vehicle-km, including indirect (rest of life cycle chain) contributions.

Conclusions

In order to improve the spatial resolution of impact assessment in a way that is simple enough to be compatible with life cycle impact assessment and scenario modelling, two new approximation methods have been developed. Firstly, an analytical approximation of the spatial distribution of cars in Europe which is in particular useful to set up future scenarios with few parameters was proposed. Secondly, an approximation for average space-dependent impact assessment interpolating continuously between analytical and numerical models was proposed.

It is expected that direct primary PM emissions are reduced in future due to stricter exhaust emission regulations. Non-exhaust emissions are expected to dominate health impacts of direct emissions from cars in 2050. Electric vehicles can contribute significantly to additional reductions of direct exhaust and non-exhaust PM emissions and health impacts particularly in densely populated areas. Using moderate assumptions on emission factors and impact estimates, an 80% electric vehicle scenario for 2050 implies an estimated additional reduction of more than 17'000 YOLL per year in the category of direct primary PM emissions from vehicles, of which more than 5'000 YOLL per year are saved due to electric braking. For the overall assessment, indirect contributions from the life cycle become more and more important. In particular the total impacts of electric vehicles depend strongly on the electricity supply chain.

Appendix: Exposure model

Firstly, a Gaussian dispersion model for a point source on flat terrain with constant diffusivities is considered. It's assumed that particles are totally absorbed when they hit the ground at z=0 (Seinfeld and Pandis 2006). The emission height $z_s>0$ is assumed to be far below the mixing layer height. The concentration field after a pulse emission of a mass *m* emitted at time $t_s=0$ from a point source at $(0,0,z_s)$ in area $\mathbf{A}_n$, is then described by (Seinfeld and Pandis 2006) ($z\geq 0$)

$$\langle c(x,y,z,t)\rangle = \frac{m}{(2\pi)^{3/2}\sigma_x\sigma_y\sigma_z}\exp\left(-\frac{(x-ut)^2}{2\sigma_x^2}-\frac{y^2}{2\sigma_y^2}\right)\cdot\left(\exp\left(-\frac{(z-z_s)^2}{2\sigma_z^2}\right)-\exp\left(-\frac{(z+z_s)^2}{2\sigma_z^2}\right)\right) \quad (7)$$

The coordinate system is chosen so that the wind moves in x direction. The wind speed u is assumed to be constant. The standard deviations σ are related to the diffusivities *K* by

$$K_{xx}=\frac{1}{2}\frac{d\sigma_x^2}{dt},\quad K_{yy}=\frac{1}{2}\frac{d\sigma_y^2}{dt},\quad K_{zz}=\frac{1}{2}\frac{d\sigma_z^2}{dt}, \quad (8)$$

in case of constant diffusivities:

$$\sigma_x^2 = \sigma_x(t)^2 = 2K_{xx} \cdot t, \quad \sigma_y^2 = \sigma_y(t)^2 = 2K_{yy} \cdot t, \quad \sigma_z^2 = \sigma_z(t)^2 = 2K_{zz} \cdot t \tag{9}$$

The dry deposition velocity is given by (Seinfeld and Pandis 2006)(18.92)

$$v_d = \frac{\partial \langle c \rangle}{\partial z} \cdot \frac{K_{zz}}{\langle c \rangle} \tag{10}$$

Taking the first order Taylor expansion around z=0 (for $z+z_s << 2\sigma_z^2$) of (7), yields an approximation for the dry deposition velocity for small z and constant diffusivity as:

$$v_d(z) \approx \frac{K_{zz}}{z} \tag{11}$$

At ground level z=0, the concentration is zero and v_d is infinite due to total absorption.

Let's consider the transition of the plume from area $\mathbf{A}_n$ with population constant density $p(\mathbf{A}_n)$ into the neighboring region $\mathbf{A}_{n,r}$ with constant population density $p(\mathbf{A}_{n,r})$ following the wind in x direction. The exposure of the population at receptor level z is (if $A_{n,r}$ is large enough, otherwise more terms have to be added in essentially the same way):

$$\begin{aligned} &\int_{-\infty}^{\infty} dx \int_{-\infty}^{\infty} dy \int_{0}^{\infty} dt\, p(x,y) \langle c(x,y,z,t) \rangle \\ &\approx p(\mathbf{A}_n) \cdot \int_{A_n} dxdy \int_{0}^{\infty} dt \langle c(x,y,z,t) \rangle + p(\mathbf{A}_{n,r}) \cdot \int_{A_{n,r}} dxdy \int_{0}^{\infty} dt \langle c(x,y,z,t) \rangle \end{aligned} \tag{12}$$

The slender plume approximation assumes that the spreading in x direction is negligible i.e. the plume moves with the wind in x direction with x=ut, u>0. Furthermore, let $x_b>0$ be the distance from the emission point to the boundary of region $\mathbf{A}_n$ in downwind direction where the population density may change. Moreover let's assume that the plume spreads out in y direction in a small angle as it is the case for the σ_y of the widely used Pasquill stability classes (Seinfeld and Pandis 2006). Then the boundary of the area in wind direction can be approximated as line $x=x_b$ and the integration over the areas can be approximated as

$$\int_{A_n} dxdy... \approx \int_{0}^{x_b} dx \int_{-\infty}^{\infty} dy... \quad , \qquad \int_{A_{n,r}} dxdy... \approx \int_{x_b}^{\infty} dx \int_{-\infty}^{\infty} dy... \tag{13}$$

The integration over t and y yields for the exposure approximately

$$\int_{-\infty}^{\infty} \int_{-\infty}^{\infty} \int_{0}^{\infty} p(x,y) \langle c(x,y,z,t) \rangle dxdydt \approx p(\mathbf{A}_n) \cdot \int_{0}^{x_b} \tilde{c}(x,z) dx + p(\mathbf{A}_{n,r}) \cdot \int_{x_b}^{\infty} \tilde{c}(x,z) dx \tag{14}$$

with

$$\tilde{c}(x,z) = \frac{m}{(2\pi)^{1/2} \cdot u \cdot \sigma_z(\frac{x}{u})} \left(\exp\left(-\frac{(z-z_s)^2}{2 \cdot (\sigma_z(\frac{x}{u}))^2} \right) - \exp\left(-\frac{(z+z_s)^2}{2 \cdot (\sigma_z(\frac{x}{u}))^2} \right) \right) \tag{15}$$

For road traffic, the emissions take place practically at the receptor level near ground i.e. it can be assumed that $z \approx z_s$ and $v_d \approx v_d(z) \approx v_d(z_s)$. Together with the functional shape of σ_z this yields

$$\int_{0}^{\infty} \tilde{c}(x,z_s) dx \approx \frac{m}{v_d} \tag{16}$$

The share of the integral over concentration inside area $\mathbf{A}_n$ is

$$\left(\int_{0}^{x_b} \tilde{c}(x,z_s) dx \right) / \left(\int_{0}^{\infty} \tilde{c}(x,z_s) dx \right) = 1 - erf\left(\sqrt{\frac{z_s u}{x_b v_d}} \right) + \sqrt{\frac{x_b}{\pi \cdot z_s} \cdot \frac{v_d}{u}} \cdot \left(1 - \exp\left(-\frac{z_s u}{x_b v_d} \right) \right) \tag{17}$$

For small x_b, the exponential tends to zero and the argument in the error function erf() tends to infinity i.e. the error function to 1, thus an approximation for the share inside area $\mathbf{A}_n$ is

$$\left(\int_0^{x_b}\widetilde{c}(x,z_s)dx\right)/\left(\int_0^{\infty}\widetilde{c}(x,z_s)dx\right)\approx\min\left(1,\left(\frac{x_b}{(\pi z_s u)/v_d}\right)^{\kappa}\right),\qquad with\ \kappa=\frac{1}{2} \tag{18}$$

The minimum function min() is used to cut off the function i.e. to keep the share between 0 and 1 (the parameters in the function are all positive). If A_n is the area of a circle and the emission point is in the center, x_b is the circle radius, i.e. $A_n=\pi*(x_b)^2$. Thus

$$\left(\int_0^{x_b}\widetilde{c}(x,z_s)dx\right)/\left(\int_0^{\infty}\widetilde{c}(x,z_s)dx\right)\approx\min\left(1,\left(\frac{A_n}{A_0}\right)^{\frac{\kappa}{2}}\right),\quad with\ \kappa=\frac{1}{2},\quad A_0=\pi\left(\frac{\pi z_s u}{v_d}\right)^2 \tag{19}$$

Eq (19) together with (14) yields (5). Alternatively, (17) can be inserted instead of (19). **Figure 11** shows the exact solution of the integral compared to the cut-off approximation as function of the area size A_n for parameters v_d=0.002m/s, z_s=1m, u=3.5m/s, $A_0\approx10^8 m^2$.

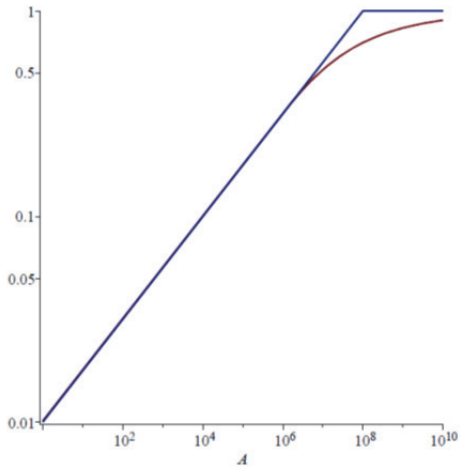

Figure 11: Share of the exposure integral inside area A (in m^2): exact integral (red) and cut-off approximation (blue).

If the area is not exactly a circle, the square root of the area is still a measure for the linear extension i.e. for an average downwind distance from a randomly chosen point inside the area to the boundary.

Including homogeneous scavenging, in a simplified way by multiplication of (7) by exp(-Λt) with a constant scavenging coefficient Λ modifies the integral from 0 to ∞ (16) into

$$\frac{m}{2\sqrt{\Lambda\cdot v_d\cdot z_s}}\left(1-\exp(-2\sqrt{\Lambda\cdot z_s/v_d})\right) \tag{20}$$

Furthermore, one may imagine random scavenging processes (e.g. rain) starting and ending at random times. If the time of emission is during a scavenging process, both the short-distance and the long-distance concentrations of the plume decrease. On the other hand, if the scavenging starts at a late time when the plume has already moved far away from the emission location, only the long-distance effects are reduced. Thus random scavenging decreases the contribution of long-distance effects relative to short-distance effects. A numeric Lagrangian dispersion model that follows an air parcel on a grid has a similar effect. Wet deposition is applied consecutively when the air parcel moves from grid cell to grid cell so that the scavenging effect sums up over long distance. Thus random scavenging tends to shift the relative distribution (**Figure 11**) more towards the cut-off function.

More generally, several commonly used analytical models can be reduced to the shape

$$\widetilde{c}(x,z)=c_0\left(\frac{1}{x^{\alpha}}\exp\left(-\frac{b_1(z)}{x^{\beta}}\right)+s\cdot\frac{1}{x^{\alpha}}\exp\left(-\frac{b_2(z)}{x^{\beta}}\right)\right) \tag{21}$$

(α>0, β>0 ,b_1>0, b_2>0, c_0>0; b_1,b_2,c_0 do not depend on x).

a) This includes the Gaussian models (Seinfeld and Pandis 2006) with

$$\sigma_z = Rx^{\alpha}, \quad \beta = 2\alpha, \quad b_1(z) = (z - z_s)^2 / 2R^2, \quad b_2(z) = (z + z_s)^2 / 2R^2$$

and with s=0 for simple Gaussian dispersion, s=1 for total reflection, s=-1 for total absorption at ground z=0.

b) It includes also the solution for a point source near the ground with height-dependent wind speed and height-dependent diffusivity (Huang 1979):

$$u(z) = \tilde{a} \cdot z^{\tilde{p}}, \quad K_{zz}(z) = \tilde{b} \cdot z^{\tilde{n}}$$

with

$$\alpha = \frac{1+\tilde{p}}{\tilde{\alpha}}, \quad \tilde{\alpha} = 2 + \tilde{p} - \tilde{n}, \quad \beta = 1, \quad b_1(z) = \frac{\tilde{a}(z^{\tilde{\alpha}} + z_s^{\tilde{\alpha}})}{\tilde{b} \cdot \tilde{\alpha}^2}, \quad s = 0$$

Again the integral over the area $\mathbf{A}_n$ i.e. x=0..x_b, is needed. The substitution

$$\tilde{x} = b_{1,2}(z) \cdot x^{-\beta} \tag{22}$$

allows for the formal integration (convergence depends on choice of parameters) and leads to

$$\int_0^{x_b} \frac{1}{x^{\alpha}} \exp\left(-\frac{b_{1,2}(z)}{x^{\beta}}\right) dx = \frac{\left(b_{1,2}(z)\right)^{\frac{1-\alpha}{\beta}}}{\beta} \int_{\frac{b_{1,2}(z)}{(x_b)^{\beta}}}^{\infty} \tilde{x}^{\left(\frac{\alpha-1}{\beta}-1\right)} \cdot \exp(-\tilde{x}) d\tilde{x}$$

$$= \frac{\left(b_{1,2}(z)\right)^{\frac{1-\alpha}{\beta}}}{\beta} \Gamma\left(\frac{\alpha-1}{\beta}, \frac{b_{1,2}(z)}{(x_b)^{\beta}}\right) \tag{23}$$

Γ is the upper incomplete gamma function (Gradshteyn et al. 1980).

Acknowledgements

This work was supported by the Competence Center Energy and Mobility (CCEM/ETH), Swisselectric Research, Erdöl-Vereinigung, and Swiss Competence Center for Energy Research (SCCER mobility).

References

Abbey, D. E., M. D. Lebowitz, P. K. Mills, F. F. Petersen, W. L. Beeson and R. J. Burchette (1995). "Long-term ambient concentrations of particulates and oxidants and development of chronic disease in a cohort of nonsmoking California residents." *Inhalation toxicology* **7**(1): 19-34.

Andre, M. (2004). "Real-world driving cycles for measuring cars pollutant emissions–Part A: The ARTEMIS European driving cycles." *Report Inrets-LTE* **411**: 97.

BAFU (2010). *Luftschadstoff-Emissionen des Strassenverkehrs 1990–2035. Aktualisierung 2010*. Umwelt-Wissen Nr. 1021. Bern, Bundesamt für Umwelt (BAFU).

Beelen, R., O. Raaschou-Nielsen, M. Stafoggia, Z. J. Andersen, G. Weinmayr, B. Hoffmann, K. Wolf, E. Samoli, P. Fischer and M. Nieuwenhuijsen (2014). "Effects of long-term exposure to air pollution on natural-cause mortality: an analysis of 22 European cohorts within the multicentre ESCAPE project." *The Lancet* **383**(9919): 785-795.

BfS (2012). *STAT-TAB Strassenfahrzeugbestand: Personenwagen 2010*. Neuchâtel Bundesamt für Statistik.

Bickel, P., R. Friedrich (eds), B. Droste-Franke, T. M. Bachmann, A. Greßmann, A. Rabl, A. Hunt, A. Markandya, R. Tol, F. Hurley, S. Navrud, S. Hirschberg, P. Burgherr, T. Heck, R. Torfs, L. de Nocker, S. Vermoote and J. Tidblad (2005). *ExternE - Externalities of Energy - Methodology 2005 Update*. Brussels, European Commission, ISBN 92-79-00423-9

Boulter, P. (2005). *Non-exhaust PM emissions: road vehicle tyre and brake wear*. 38th IAPSC Conference. 16th June. London.

Brunekreef, B. and S. T. Holgate (2002). "Air pollution and health." *The lancet* **360**(9341): 1233-1242.

Bukowiecki, N., R. Gehrig, P. Lienemann, M. Hill, R. Figi, B. Buchmann, M. Furger, A. Richard, C. Mohr, S. Weimer, A. Prévôt and U. Baltensperger (2009). *PM10 emission factors of abrasion particles from road traffic. Report*, EMPA/PSI Bundesamtes für Strassen (ASTRA).

Cadle, S. H. (2004). *On-Road Mobile Source PM and Black Carbon Emission Rates*. Black Carbon Emissions and Climate Change Workshop. San Diego.

Curtiss, P. and A. Rabl (1996). "Impacts of air pollution: general relationships and site dependence." *Atmospheric Environment* **30**(19): 3331-3347.

Derwent, R. G. and K. Nodop (1986). "Long-range Transport and Deposition of Acidic Nitrogen Species in North-west Europe." *Nature* **324**: 356-358.

DIW (2012). *Wochenbericht Nr.47*, DIW.

Dockery, D. W., C. A. Pope, X. Xu, J. D. Spengler, J. H. Ware, M. E. Fay, B. G. Ferris Jr and F. E. Speizer (1993). "An association between air pollution and mortality in six US cities." *New England journal of medicine* **329**(24): 1753-1759.

Droste-Franke, B., T. Heck, J. Karnahl, W. Krewitt, D. Malthan, P. Mayerhofer, F. Pattermann, S. Schmid, A. Trukenmüller, R. Ungermann, P. Bickel and R. Friedrich (2004). *EcoSense 4.0, User's Manual*. Stuttgart, IER, University of Stuttgart.

Ecoinvent (2010). *database v2.2*.

EMEP (1996). *EMEP MSC-W Report 1/96*. Oslo, Norway, The Norwegian Meteorological Institute.

EMEP/CORINAIR (2007). *Atmospheric Emission Inventory Guidebook. Technical report No 16/2007*, European Environment Agency (EEA).

Eurostat (2012). *Transport in figures*, European Commission Directorate-General for Mobility and Transport.

Eurostat (2014). *Stock of vehicles by category and NUTS 2 regions [tran_r_vehst]*.

Friedrich, R. and P. Bickel, Eds. (2001). *Environmental External Costs of Transport*. Berlin, Springer.

Garg, B. D., S. H. Cadle, P. A. Mulawa, P. J. Groblicki, C. Laroo and G. A. Parr (2000). "Brake wear particulate matter emissions." *Environmental Science & Technology* **34**(21): 4463-4469.

Gollnick, V. (2004). *Untersuchungen zur Bewertung der Transporteffizienz verschiedener Verkehrsmittel*, Universität München.

Götschi, T., J. Heinrich, J. Sunyer and N. Künzli (2008). "Long-term effects of ambient air pollution on lung function: a review." *Epidemiology* **19**(5): 690-701.

Gradshteyn, I. S., I. M. Ryzhik, A. Jeffrey and Y. V. Geronimus (1980). *Table of integrals, series, and products*. New York, Academic Press, ISBN 0-12-294760-6

Heck, T. and S. Hirschberg (2011). China: Economic impacts of air pollution in the country. *Encyclopedia of Environmental Health*. J. O. Nriagu. Burlington, Elsevier. **1:** 625–640

Heck, T., W. Krewitt, D. Malthan, P. Mayerhofer, F. Pattermann, A. Trukenmüller, R. Ungermann and R. Friedrich (1999). *EcoSense 2.0, User's Manual*. Stuttgart, IER, University of Stuttgart.

Heck, T. and N. K. Meyer (2010). *External costs related to impacts of biomass combustion systems*. CCES Latsis Symposium, ETH Zürich.

Holland, M., J. Berry, D. Forster (eds), P. Watkiss, R. Boyd, D. Lee, T. Schneider, C. Scheiber, V. Tort, M. Dreicer, J. Montes, P. Linares, A. Prades, G. Atkinson, D. McCoy, A. Rabl, P. Curtiss, J. V. Spadaro, T. Downing, N. Eyre, L. Eeckhoudt, W. Krewitt, R. Friedrich, A. Greßmann, P. Mayerhofer, T. Heck, A. Trukenmüller, F. Hurley, P. Donnan, B. Miller, A. Pilkington, M. Hornung, H. Jones, D. Howard, G. Howson, U. Rosengren-Brinck, R. Tol, A. Markandya, I. Milborrow, B. Lockwood, S. Ascari, M. Bernasconi, K. Rennings, I. Kuhn and H. Wiggering (1999). *ExternE - Externalities of Energy. Volume 7: Methodology 1998 update*. Brussels, European Commission, ISBN 92-828-7782-5

Huang, C. (1979). "A theory of dispersion in turbulent shear flow." *Atmospheric Environment* **13**(4): 453-463.

Hurley, F., A. Hunt, H. Cowie, M. Holland, B. Miller, S. Pye and P. Watkiss (2005). "Methodology for the cost-benefit analysis for CAFE: volume 2: health impact assessment." *Didcot. UK: AEA Technology Environment*.

Jensen, S. S., E. Willumsen, J. Brandt and N. B. Kristensen (2008). "Evaluation of exposure factors applied in marginal external cost analysis of transportation related air pollution." *Transportation Research Part D: Transport and Environment* **13**(4): 255-273.

Krewitt, W., A. Trukenmüller, T. M. Bachmann and T. Heck (2001). "Country-Specific Damage Factors for Air Pollutants. A Step Towards Site Dependent Life Cycle Impact Assessment." *International Journal of Life Cycle Assessment* **6**: 199-210.

Laden, F., L. M. Neas, D. W. Dockery and J. Schwartz (2000). "Association of fine particulate matter from different sources with daily mortality in six US cities." *Environmental health perspectives* **108**(10): 941.

Moussiopoulos, N., I. Douros, G. Tsegas, E. Chourdakis and S. T. Ortiz (2012). "An approach for determining urban concentration increments." *International Journal of Environment and Pollution* **50**(1): 376-385.

NEEDS (2009). *New Energy Externalities Developments for Sustainability*.

Ostro, B. D. (1987). "Air pollution and morbidity revisited: a specification test." *Journal of Environmental Economics and Management* **14**(1): 87-98.

Pope III, C. A. and D. W. Dockery (2006). "Health effects of fine particulate air pollution: lines that connect." *Journal of the Air & Waste Management Association* **56**(6): 709-742.

Pope III, C. A., M. Ezzati and D. W. Dockery (2009). "Fine-particulate air pollution and life expectancy in the United States." *New England Journal of Medicine* **360**(4): 376-386.

Raaschou-Nielsen, O., Z. J. Andersen, R. Beelen, E. Samoli, M. Stafoggia, G. Weinmayr, B. Hoffmann, P. Fischer, M. J. Nieuwenhuijsen and B. Brunekreef (2013). "Air pollution and lung cancer incidence in 17 European cohorts: prospective analyses from the European Study of Cohorts for Air Pollution Effects (ESCAPE)." *The lancet oncology* **14**(9): 813-822.

Schindler, C., D. Keidel, M. W. Gerbase, E. Zemp, R. Bettschart, O. Brandli, M. H. Brutsche, L. Burdet, W. Karrer and B. Knopfli (2009). "Improvements in PM10 exposure and reduced rates of respiratory symptoms in a cohort of Swiss adults (SAPALDIA)." *American journal of respiratory and critical care medicine* **179**(7): 579-587.

Schmid, S. A. (2005). *Externe Kosten des Verkehrs: Grenz-und Gesamtkosten durch Luftschadstoffe und Lärm in Deutschland. Dissertation*. Stuttgart, University of Stuttgart, ISBN

Seinfeld, J. H. and S. N. Pandis (2006). *Atmospheric chemistry and physics: from air pollution to climate change*, John Wiley & Sons, ISBN 1118591364

Simons, A. (2013). "Road transport: new life cycle inventories for fossil-fuelled passenger cars and non-exhaust emissions in ecoinvent v3." *The International Journal of Life Cycle Assessment*: 1-15.

Skinner, I., H. van Essen, R. Smokers and N. Hill (2010). *Towards the decarbonisation of the EU's transport sector by 2050*. Brussels, European Commission Directorate-General Environment and AEA Technology.

Spadaro, J. V. (1999). *Quantifying the effects of airborne pollution: impact models, sensitivity analyses and applications*. Ecole des Mines, Paris.

Spielmann, M., C. Bauer, R. Dones and M. Tuchschmid (2007). "Transport Services. ecoinvent report No. 14." *Swiss Centre for Life Cycle Inventories, Dübendorf*.

Torfs, R., F. Hurley, B. Miller and A. Rabl (2007). *Deliverable 3.7-RS1b/WP3 "A set of concentration-response functions"*, European Commission - NEEDS project.

Torras Ortiz, S. (2012). *A hybrid dispersion modelling approach for quantifying and assessing air quality in Germany with focus on urban background and kerbside concentrations*. IER, University of Stuttgart.

Torras Ortiz, S. and R. Friedrich (2013). "A modelling approach for estimating background pollutant concentrations in urban areas." *Atmospheric Pollution Research* **4**: 147-156.

Trukenmüller, A. and R. Friedrich (1995). Die Abbildung der großräumigen Verteilung, chemischen Umwandlung und Deposition von Luftschadstoffen mit dem Trajektorienmodell WTM. *Jahresbericht ALS*. Stuttgart**:** 93 – 108.

VSS (2009). *Norm SN 641828 - Externe Kosten*. Zürich, Schweizerischer Verband der Strassen- und Verkehrsfachleute.

Xu, X. (1998). Air pollution and its health effects in urban China. *Energizing China*. M. McElroy, C. Nielson and P. Lydon. Cambridge, MA, Harvard University Press.